

# Metamagnetism of the manganese subsystem in $\text{RMn}_2$ intermetallic compounds

I. Yu. Gaidukova, S. B. Kruglyashov, A. S. Markosyan, R. Z. Levitin,  
Yu. G. Pastushenkov, and V. V. Snegirev

Moscow State University

(Submitted 26 November 1982)

Zh. Eksp. Teor. Fiz. **84**, 1858–1867 (May 1983)

The results of an investigation in the temperature range 5.5–300 K of the magnetic properties and crystal structure of  $\text{RMn}_2$  intermetallic compounds having the  $C 15$  cubic structure ( $R = \text{Gd, Tb, or Dy}$ ) or the  $C 14$  hexagonal structure ( $R = \text{Ho, Er, or Tm}$ ) are presented. It is shown that whereas the transition to the magnetically ordered state is second order for  $R = \text{Dy, Ho, Er, and Tm}$ , for  $R = \text{Gd and Tb}$  it is a first order transition with a discontinuous increase in the volume of the unit cell ( $\Delta V/V \approx 15 \times 10^{-3}$  at 5.5 K). It is concluded that this behavior of  $\text{GdMn}_2$  and  $\text{TbMn}_2$  is related to the magnetic ordering of the manganese subsystem, which is of metamagnetic type. In the other  $\text{RMn}_2$  compounds the exchange field acting on the manganese subsystem from the rare earth sublattice is weaker, so the manganese sublattice does not become ordered. The results are compared with the behavior of the  $3d$  subsystem in similar  $\text{RM}_2$  compounds with  $M = \text{Fe, Co, and Ni}$ .

PACS numbers: 75.30.Kz, 75.25.+z, 75.50.Ee, 61.55.Hg

## INTRODUCTION

The interest manifested in recent years in intermetallic compounds of the type  $\text{RM}_2$ , where  $R$  is a rare earth (RE) element and  $M$  is a  $3d$  transition metal, is due to the fact that these compounds reveal a complex interaction of two magnetic subsystems—the RE and  $3d$ -metal subsystems. Whereas the first subsystem is described by the localized-moment model, most investigators believe that the magnetism of the second subsystem is due to collectivization of the carriers.<sup>1,2</sup> The essential feature is that, in a number of cases, the magnetization of the  $3d$  subsystem exhibits metamagnetic behavior.<sup>3,4</sup>

The ideas mentioned above were developed on the basis of studies of intermetallic compounds of RE elements with Fe, Co, or Ni. The  $\text{RMn}_2$  compounds have been considerably less intensively studied. This is due mainly to technical difficulties that arise on account of the high vapor pressure of molten manganese. The comparatively few available studies<sup>2,5–8</sup> of these compounds indicate that they are magnetically ordered at low temperatures. However, there is a wide spread between the values obtained in different studies for the magnetic ordering temperature, the saturation magnetic moments, etc., and the extent to which the ideas advanced concerning the nature of the magnetic ordering in  $\text{RM}_2$  compounds with  $M = \text{Ni, Co, and Fe}$  can be extended to  $\text{RMn}_2$  compounds has not been analyzed at all. To clarify this situation we have investigated the magnetic properties of the  $\text{RMn}_2$  intermetallic compounds with  $R = \text{Gd, Tb, Dy, and Ho}$ , and have also investigated the crystal structure of these compounds and of  $\text{ErMn}_2$  and  $\text{TmMn}_2$ .

## MEASUREMENT TECHNIQUE AND SPECIMENS

We measured the magnetizations and susceptibilities over the temperature range 4.2–350 K in the field of a superconducting solenoid at field strengths up to 60 kOe, using a vibration magnetometer. The measurement errors did not exceed 3%. The crystal structures were investigated over the

temperature range 5.5–300 K using a diffractometer with a low-temperature attachment. The measurements were made on polycrystalline specimens smelted in an electric arc or induction furnace in an argon atmosphere.<sup>9</sup> The phase composition of the specimens was monitored by x-ray diffraction. Specimens intended for magnetic measurements were subjected, in addition, to a metallographic analysis. The impurity-phase concentration in the investigated specimens did not exceed 1%.

## EXPERIMENTAL RESULTS

In accordance with the results of other studies,<sup>2,7</sup> at room temperature the synthesized  $\text{RMn}_2$  compounds with  $R = \text{Gd, Tb, and Dy}$  have a cubic crystal structure like that of the Laves phase of  $\text{MgCu}_2$  ( $C 15$ ), and those with  $R = \text{Ho, Er, and Tm}$  have a hexagonal structure like that of the Laves phase of  $\text{MgZn}_2$  ( $C 14$ ).

Figure 1 shows the temperature dependences of the magnetization and reciprocal susceptibility for several  $\text{RMn}_2$  compounds. The susceptibility obeys the Curie-Weiss law at high temperatures. The paramagnetic Curie point  $\theta_p$  decreases on going from  $\text{GdMn}_2$  to  $\text{HoMn}_2$  (see Table I). It is also evident from this table that the experimental effective magnetic moments  $\mu_{\text{eff}}$  of the investigated  $\text{RMn}_2$  compounds are somewhat higher than those of the free  $\text{R}^{3+}$  ions; this may be attributed to the contribution of the manganese subsystem to the paramagnetic susceptibility.

Figure 2 shows the magnetization isotherms at 4.2 K of the investigated specimens.  $\text{GdMn}_2$ ,  $\text{DyMn}_2$ , and  $\text{HoMn}_2$  already reach saturation in 15–30-kOe fields, whereas  $\text{TbMn}_2$  remains unsaturated even at 60 kOe.<sup>11</sup> The fact that  $\text{TbMn}_2$  remains unsaturated may be due to its high magnetic anisotropy; indeed, the fact that  $\text{TbMn}_2$ , unlike the other investigated compounds, retains its maximum magnetization below  $T_C$  even in a 60-kOe field (Fig. 1) indicates that this may be the case.

TABLE I. Magnetic characteristics of  $\text{RMn}_2$  inter-metallic compounds.

$\text{RMn}_2$	$\mu_S(4.2^\circ\text{K}), \mu_B$	$\mu_{\text{R theor}} = gJ, \mu_B$	$\mu_{\text{Mn}}, \mu_B$	$\mu_{\text{R eff theor}} = g(J+1)J/\mu$	$\mu_{\text{eff theor}}, \mu_B$	$\Theta_p, ^\circ\text{K}$	$T_C, ^\circ\text{K}$	Order of the magnetic phase transition
$\text{GdMn}_2$	2.7	7.0	2.15	7.94	8.4	100	110	I
$\text{TbMn}_2$	$\sim 5.0^*$	9.0	$\leq 2.00$	9.72	9.45	70	26	I
$\text{DyMn}_2$	7.1	10.0	$\leq 1.45$	10.65	11.3	40	49	II
$\text{HoMn}_2$	8.7	10.0	$\leq 0.65$	10.61	11.8	18	31	II

\*In a 55 kOe field.

The saturation magnetic moments  $\mu_S$  for the intermetallic compounds  $\text{RMn}_2$  are given in Table I. The value given for  $\text{TbMn}_2$  is only an estimate. It is evident from Table I that for all the investigated compounds  $\mu_S$  is lower than the magnetic moment of the corresponding free RE ion. This difference is especially noticeable in the case of  $\text{GdMn}_2$  and  $\text{TbMn}_2$ . Assuming that the nature of the magnetic interaction in  $\text{RMn}_2$  compounds is the same as in other  $\text{RM}_2$  compounds with heavy RE metals (a positive R-R exchange interaction leading to parallel orientation of the RE moments and a negative R-d interaction leading to antiparallel orientation of the RE and d moments<sup>1</sup>), we find that the magnetic moment per manganese ion in  $\text{RMn}_2$  compounds is

$$\mu_{\text{Mn}} = 1/2 (\mu_S - \mu_{\text{R}}). \quad (1)$$

For such calculations one must know the magnetic moment  $\mu_{\text{R}}$  of the RE ion which, in the case of RE ions having a nonzero orbital angular momentum may be smaller than

$gJ\mu_B$  because of the effect of the crystal field. Only in the case of Gd, therefore, which is in an S state ( $L = 0$ ) so that the effects of the crystal field can be neglected, is it possible to determine  $\mu_{\text{Mn}}$  from the data obtained:  $\mu_{\text{Mn}} = 2.15\mu_B$ . For the other investigated intermetallic  $\text{RMn}_2$  compounds we can only estimate  $\mu_{\text{Mn}}$  from above (see Table I). Such an estimate is made more plausible by data of NMR studies,<sup>10</sup> which yield the value  $\mu_{\text{Mn}} = 0.4\mu_B$  for the cubic modification of  $\text{HoMn}_2$ , and by neutron diffraction data,<sup>11</sup> which yield  $\mu_{\text{Mn}} \approx 0.8\mu_B$  in the cubic and hexagonal modifications of  $\text{HoMn}_2$  (in the hexagonal modification, this is the average moment of manganese in inequivalent positions).

We used the method of thermodynamic coefficients<sup>12</sup> to determine the magnetic transition temperatures for the intermetallic compounds  $\text{DyMn}_2$  and  $\text{HoMn}_2$ . The resulting data are given in Table I. It follows from our measurements, however, that the magnetization isotherms for  $\text{GdMn}_2$  and  $\text{TbMn}_2$  are not represented near the transition point by the formula  $H/\mu = \alpha + \beta\mu^2$ , which follows from the thermodynamic theory of second order magnetic phase transitions. For these compounds we used susceptibility measurements in weak fields ( $\sim 30$  Oe) to determine  $T_C$ . It is evident from Fig. 3 that the magnetic transition in  $\text{GdMn}_2$  takes place at  $\sim 110$  K and exhibits considerable hysteresis. This, as well as crystal structure data (see below), indicates that the magnetic transition in this compound is of first order. Contradictory data on the magnetic properties of  $\text{GdMn}_2$  have been published in recent years; in particular, the Curie tempera-

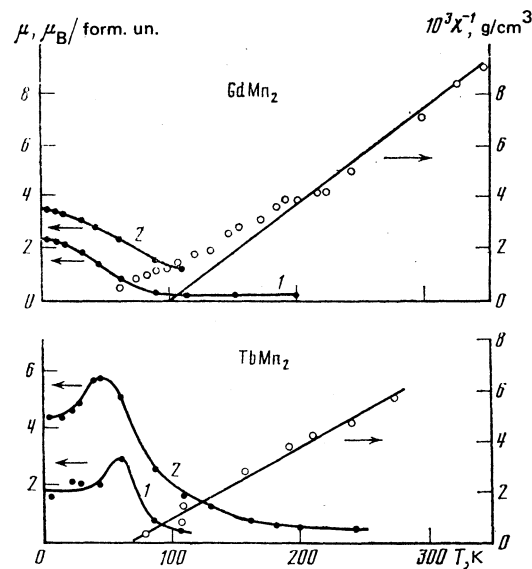


FIG. 1. Temperature dependences of the reciprocal susceptibility  $\chi^{-1}$  and magnetization  $\mu$ ; for  $\text{GdMn}_2$  in 5 kOe (1) and 40 kOe (2) fields and for  $\text{TbMn}_2$  in 10 kOe (1) and 40 kOe (2) fields.

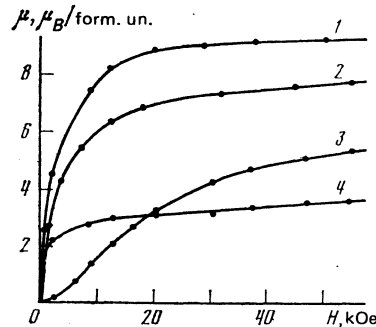


FIG. 2. Magnetization isotherms for  $\text{RMn}_2$  compounds at 4.2 K: 1— $\text{HoMn}_2$ , 2— $\text{DyMn}_2$ , 3— $\text{TbMn}_2$ , 4— $\text{GdMn}_2$ .

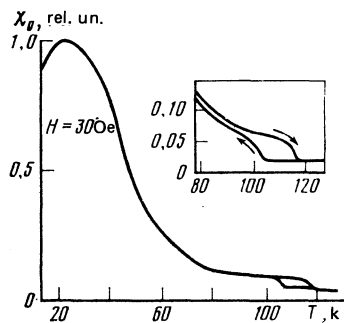


FIG. 3. Initial susceptibility  $\chi_0$  for  $\text{GdMn}_2$ . The inset shows the transition region on a larger scale.

ture is given as 38, 86, 185, and 283 K in Refs. 7, 2, 13, and 8, respectively. A discontinuity in the initial susceptibility at 110 K was noted in Ref. 8, but this temperature was not interpreted as the transition point to the magnetically ordered state. The contradictory data might be due to the presence of small quantities of strongly magnetic impurities (for example, Gd and intermetallic compounds of it that differ stoichiometrically from  $\text{GdMn}_2$ ). Some of our data also suggest this interpretation: we observed a small spontaneous magnetization even above  $T_C = 110$  K in some specimens. Errors due to inaccuracies in determining  $T_C$  from data on temperature dependences of the magnetization in a field, as was done in Refs. 7 and 13, are also possible.

It follows from measurements of the temperature dependence of the susceptibility of  $\text{TbMn}_2$  in weak fields that the magnetic transition in this compound is also a first order phase transition and takes place at 26 K.<sup>2)</sup> This is also confirmed by crystal-structure data (see below). That the phase transition at  $T_C$  in  $\text{TbMn}_2$  is of first order is also indicated by the unusual behavior of the magnetization above the transition point in the temperature range 26–50 K. Figure 4 shows typical  $\mu(H)$  curves for this compound at various temperatures in the ordered region (below 25 K), the transition region (26–50 K), and the paramagnetic region (above 50 K). In weak fields up to 10 kOe the magnetization in the transition

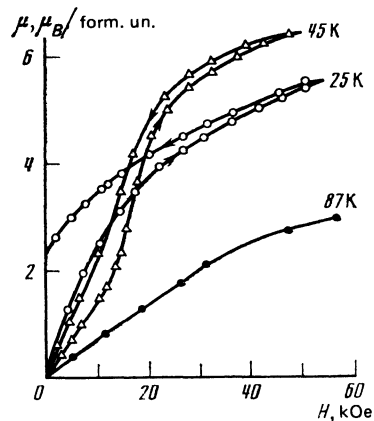


FIG. 4. Magnetization curves for  $\text{TbMn}_2$  in the ordered (25 K), metamagnetic (45 K); and paramagnetic (87 K) regions.

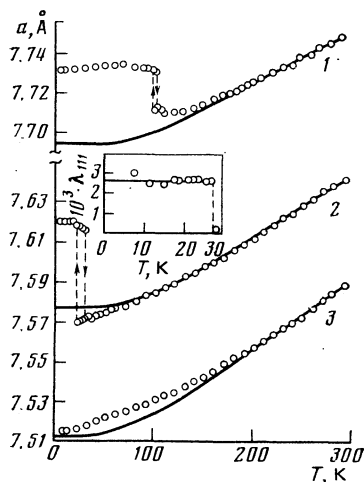


FIG. 5. Temperature dependence of the lattice constant  $a$  for cubic  $\text{RMn}_2$  compounds: 1— $\text{GdMn}_2$ , 2— $\text{TbMn}_2$ , 3— $\text{DyMn}_2$ . The points represent experimental data and the curves show the phonon contribution. The inset shows the temperature dependence of the anisotropic magnetostriction constant  $\lambda_{111}$  for  $\text{TbMn}_2$ .

region varies linearly with the field strength. When the field strength is further increased, the magnetization rises sharply. Hysteresis is also observed on the  $\mu(H)$  curve. All this indicates that the magnetization of  $\text{TbMn}_2$  is of metamagnetic type in the temperature region under discussion.

The data from the magnetic measurements do not enable us to draw final conclusions concerning the nature of the ordering of the manganese subsystem in the  $\text{RMn}_2$  compounds. Crystal-structure studies of these compounds at various temperatures can yield useful information.

Figure 5 shows the temperature dependences of the lattice constants of the cubic  $\text{RMn}_2$  compounds ( $R = \text{Gd}, \text{Tb}, \text{and Dy}$ ). Here the full curves represent the theoretical dependences in the Debye theory approximation without allowance for the magnetic interactions (the phonon contribution to the thermal expansion). The curves were calculated for the Debye temperature  $\Theta_D = 270$  K.<sup>6</sup> In the high-temperature region the  $a(T)$  curve has the normal trend, i.e., it falls monotonically with decreasing temperature. However, in  $\text{GdMn}_2$  and  $\text{TbMn}_2$  there is observed a discontinuity

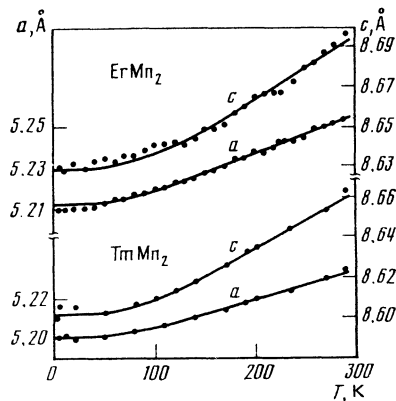


FIG. 6. Temperature dependence of the lattice constants  $a$  and  $c$  for hexagonal  $\text{RMn}_2$  compounds. The points represent experimental data and the curves show the phonon contribution.

TABLE II. Structural characteristics of RMn<sub>2</sub> compounds.

RMn <sub>2</sub>	Structure	a, Å	c, Å	$\frac{\Delta V}{V}$	$\alpha_a \cdot 10^6$	$\alpha_c \cdot 10^6$
					at 290 K	
GdMn <sub>2</sub>	Cubic	7.748	—	$14.7 \cdot 10^{-3}$	34	—
TbMn <sub>2</sub>	»	7.648	—	$15.3 \cdot 10^{-3}$	40	—
DyMn <sub>2</sub>	»	7.590	—	$<10^{-4}$	47	—
HoMn <sub>2</sub>	Hexagonal	5.330	8.600	$<10^{-4}$	43	36
ErMn <sub>2</sub>	»	5.255	8.695	$<10^{-4}$	37	36
TmMn <sub>2</sub>	»	5.238	8.660	$<10^{-4}$	29	33

$\alpha_a$  and  $\alpha_c$  are the thermal expansion coefficients along the *a* and *c* axes

uous decrease in the volume of the unit cell ( $\Delta V/V \approx 15 \times 10^{-3}$ ) near the magnetic ordering temperature, which indicates that in these compounds the magnetic transition is first order.

In addition, the magnetically ordered phase of TbMn<sub>2</sub> exhibits a rhombohedral distortion of the crystal structure. The magnitude  $\varepsilon$  of this distortion (the deviation from 90° of the angle between edges of a cube) amounts to  $2.8 \times 10^{-3}$  rad at 8 K. As has been repeatedly shown,<sup>14-16</sup> such distortions arise in RE laves phases as a result of strong anisotropic magnetoelastic interactions of single-ion nature and lead to deformation of the crystal lattice along the easy magnetization axis. In the case of TbMn<sub>2</sub>, rhombohedral distortion (deformation along the  $\langle 111 \rangle$  diagonal of the cube) indicates that the (111) direction is that of the easy axis. The inset in Fig. 5 shows the temperature dependence of the anisotropic magnetostriction constant  $\lambda_{111}$  for TbMn<sub>2</sub> in the magnetically ordered region. In accordance with the nature of the magnetic phase transition, it goes discontinuously to zero at  $T_C$ .

Unlike GdMn<sub>2</sub> and TbMn<sub>2</sub>, DyMn<sub>2</sub> exhibited no appreciable bulk anomalies of the crystal structure on passing through the Curie point. It should also be noted that there are no distortions of the cubic structures of GdMn<sub>2</sub> and DyMn<sub>2</sub> in the magnetically ordered region; this indicates that the anisotropic magnetostriction of these compounds is comparatively weak ( $< 10^{-4}$ ).

The lattice constants of hexagonal HoMn<sub>2</sub>, ErMn<sub>2</sub>, and TmMn<sub>2</sub> also exhibit no anomalies of any sort in the investigated temperature interval. Figure 6 shows the results for ErMn<sub>2</sub> and TmMn<sub>2</sub>, whose Curie points, as determined from neutron diffraction measurements, are 25 and 12 K, respectively.<sup>17</sup> The phonon contribution was calculated at  $\Theta_D = 270$  K for the lattice constant *a* and at  $\Theta_D = 350$  K for the lattice constant *c*. The lattice constants of HoMn<sub>2</sub> behave in a similar manner as the temperature is varied.

Some of the data from x-ray measurements of the RMn<sub>2</sub> compounds are summarized in Table II. The thermal expansion coefficients  $\alpha$  for the RMn<sub>2</sub> compounds are three to four times larger than those for other RM<sub>2</sub> compounds (with *M* = Ni or Co)<sup>9,16</sup>; this shows how unstable the crystal structure of the RMn<sub>2</sub> compounds is. The thermal expansion coefficient  $\alpha$  reaches its largest value at the transition from the C 15 to the C 14 structure (between DyMn<sub>2</sub> and HoMn<sub>2</sub>). This

leads to the instability of the crystal structure of HoMn<sub>2</sub>, which exists in two modifications: hexagonal and cubic.<sup>2</sup> The deviation of the temperature dependence of the lattice constant of DyMn<sub>2</sub> from the Debye law, which can be interpreted as a temperature dependence of  $\Theta_D$ , is also associated with the low stability of the crystal structure of that compound.

## DISCUSSION

Thus, our magnetic and x-ray studies have shown that the RMn<sub>2</sub> compounds can be separated into two groups. In one of the groups (comprising GdMn<sub>2</sub> and TbMn<sub>2</sub>) the transition to the magnetically ordered state is as a first order phase transition and is accompanied by gigantic magnetic bulk anomalies. In the other group (DyMn<sub>2</sub>, HoMn<sub>2</sub>, ErMn<sub>2</sub>, and TmMn<sub>2</sub>) the magnetic bulk anomalies are considerably smaller and the transition at the Curie point is first order. The observed features of the magnetic ordering of RMn<sub>2</sub> compounds have much in common with the properties of the RM<sub>2</sub> intermetallic compounds with *M* = Fe, Co, or Ni. Thus, in the RCo<sub>2</sub> series the magnetic transition is first order and is also accompanied by considerable ( $\sim 5 \times 10^{-3}$ ) bulk anomalies.<sup>3,9,18</sup> The  $\mu(H)$  curves for these compounds are of metamagnetic type above the Curie point.<sup>19</sup>

As was already noted, the magnetic behavior of the RM<sub>2</sub> compounds can be well described under the assumption that two magnetic subsystems, one formed by the localized moments of the 4*f* electrons of the rare earths (localized RE magnetism) and the other consisting of a magnetic moment of band origin produced by the 3*d* electrons of the transition metal (*d* band magnetism), coexist within them.<sup>3</sup> In Laves phases the magnetic moments of the rare earths are always ordered at low temperatures, whereas the magnetic moment of the *d* subsystem depends on structural features and on the population of the *d* band formed by the partial overlap of the 3*d* band of the transition metal, which is comparatively narrow ( $\sim 4$  eV) and has a high density of states, with the higher-energy 5*d* band of the Re metals, which is broader ( $\sim 7$  eV) and has a low density of states.<sup>4</sup> Figure 7 shows a schematic density-of-states curve  $N(\varepsilon)$  for the *d* band of RM<sub>2</sub> compounds together with the position of the Fermi level for ferromagnetic, metamagnetic, and paramagnetic behavior of the *d* subsystem.

As is well known, according to the band model the Stoner criterion

$$IN(\epsilon_F) \geq 1 \quad (2)$$

(where  $I$  is the exchange interaction integral for the band  $d$  electrons and  $N(\epsilon_F)$  is the density of states at the Fermi level) must be satisfied in order for ferromagnetism to arise. If  $N(\epsilon_F)$  is large enough (position 1 in Fig. 7) the Stoner criterion will be satisfied as a result of the  $d$ - $d$  exchange interaction, the  $3d$  subsystem will be spontaneously magnetized, and the effective field  $H_{\text{eff}}$  from the RE subsystem will increase the magnetic moment only slightly. According to Ref. 4, such a situation obtains in the  $\text{RFe}_2$  compounds (see curve 1 in Fig. 8).

In the  $\text{RNi}_2$  compounds the  $d$  band is almost completely filled (position 2 in Fig. 7), the density of states at the Fermi level is low, and magnetic ordering of the  $d$  electrons does not take place in the field  $H_{\text{eff}}$  (curve 2 in Fig. 8).

The intermediate case, which is realized in the  $\text{RCO}_2$  compounds,<sup>4</sup> is the most interesting. In these compounds the Fermi level of the  $d$  electrons lies on the steeply falling part of the  $N(\epsilon)$  curve (case 3 in Fig. 7), the density of states at the Fermi level is higher than in  $\text{RNi}_2$ , but the Stoner criterion for  $d$ - $d$  interaction is not satisfied ( $IN(\epsilon_F) \approx 0.85$ ).<sup>4</sup> The compounds  $\text{YCo}_2$  and  $\text{LuCo}_2$ , which contain nonmagnetic elements, are therefore exchange-enhanced Pauli paramagnets. In  $\text{RCO}_2$  compounds containing magnetic rare earths an additional effective field  $H_{\text{eff}}$  due to the  $f$ - $d$  exchange interaction acts on the cobalt subsystem. This reduces the energy of the subband spin-up (along the field) electrons and increases that of the spin-down (against the field) electrons (see the inset in Fig. 7). Then since the Fermi level lies on the falling part of the  $N(\epsilon)$  curve ( $N'(\epsilon_F) < 0$  and  $N''(\epsilon_F) > 0$ ), the average density of states  $N(\epsilon_F) = (N_+(\epsilon_F) + N_-(\epsilon_F))/2$  increases with increasing  $H_{\text{eff}}$  (see the inset in Fig. 7). There is a critical field strength  $H_{\text{cr}}$  above which the Stoner criterion is satisfied and the  $d$  subsystem undergoes a discontinuous transition to the magnetically ordered state, the magnetic moment of the  $d$  subsystem behaving in a metamagnetic manner as shown by curve 3 in Fig. 8.

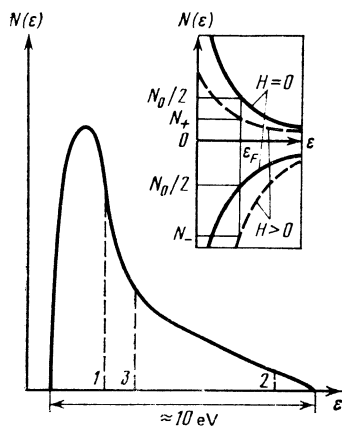


FIG. 7. Schematic density of states curve  $N(\epsilon)$  for the  $d$  subsystem of  $\text{RM}_2$  compounds, and the position of the Fermi level: 1— $\text{M} = \text{Fe}$ , ferromagnetic state; 2— $\text{M} = \text{Ni}$ , paramagnetic state; 3— $\text{M} = \text{Co}$ , metamagnetic state. The inset shows the change in  $N(\epsilon_F)$  when a field is applied.

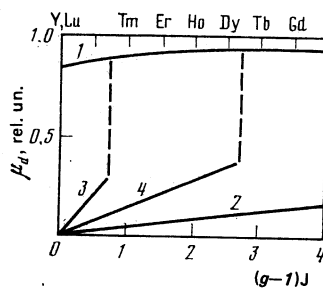


FIG. 8. Schematic depiction of the dependence on  $(g-1)J \propto H_{\text{eff}}$  of the magnetic moment  $\mu_d$  of the  $3d$  subsystem in  $\text{RM}_2$  compounds: 1— $\text{M} = \text{Fe}$ , 2— $\text{M} = \text{Ni}$ , 3— $\text{M} = \text{Co}$ , 4— $\text{M} = \text{Mn}$ .

As a result of the metamagnetic character of the magnetization of the  $d$  subsystem, the transition to the magnetically ordered state at the Curie point in the  $\text{RM}_2$  compounds becomes a first order phase transition. This situation is realized in the  $\text{RCO}_2$  compounds with  $\text{R} = \text{Dy}$ ,  $\text{Ho}$ ,  $\text{Er}$ , and, apparently,  $\text{Tm}$ .<sup>3</sup> We note that, as calculations show, a first order phase transition arises when the  $\text{R}$ - $d$  exchange interaction is dominant and the  $\text{R}$ - $\text{R}$  interaction is weak. In the opposite case the phase transition to the magnetically ordered state becomes second order. This may be one reason why the transitions to the magnetically ordered state in  $\text{GdCo}_2$  and  $\text{TbCo}_2$  are second order, for  $\text{Gd}$  and  $\text{Tb}$  have the strongest  $\text{R}$ - $\text{R}$  exchange interactions of all the rare earths.

Under the assumption of the spin character of the  $f$ - $d$  exchange, the effective field acting on the  $d$  subsystem is related to the  $g$  factor and principal quantum number  $J$  of the rare earth by the formula

$$H_{\text{eff}} \propto (g-1)J \quad (3)$$

and increases on going from  $\text{Tm}$  to  $\text{Gd}$ .  $H_{\text{eff}} > H_{\text{cr}}$  in the  $\text{RCO}_2$  compounds—even in  $\text{TmCo}_2$ —so the cobalt subsystem is magnetically ordered in all the  $\text{RCO}_2$  compounds with heavy rare earths  $\text{R}$  (curve 3 in Fig. 8).

The  $d$  subsystem band metamagnetism model is also useful in discussing the magnetic properties of the  $\text{RMn}_2$  compounds. In all cases magnetic ordering of the  $d$  subsystem in  $\text{R}$ - $3d$  intermetallides is accompanied by gigantic volume effects.<sup>9,18</sup> Moreover, ordering of the  $\text{R}$  subsystem alone does not give rise to such anomalies.<sup>16,20</sup> Among the  $\text{RMn}_2$  compounds volume anomalies are observed only in those containing  $\text{Tb}$  or  $\text{Gd}$ , and one may conclude that the manganese subsystem is ordered only in  $\text{TbMn}_2$  and  $\text{GdMn}_2$  in which, according to (3), the effective field acting from the  $\text{RE}$  sublattice is the strongest. In the other  $\text{RMn}_2$  compounds the effective field is weaker than  $H_{\text{cr}}$  and is incapable of ordering the manganese subsystem (curve 4 in Fig. 8).

Let us estimate  $H_{\text{cr}}$  for the  $\text{RMn}_2$  compounds, assuming that the structure of the  $3d$  band is the same in all these compounds. When  $H < H_{\text{cr}}$  we have, according to the model under consideration,

$$\mu_{\text{Mn}} = \chi_{\text{Mn}} H_{\text{eff}}, \quad (4)$$

where  $\chi_{\text{Mn}}$  is the paramagnetic susceptibility of  $\text{YMn}_2$  and is equal to  $1.28 \times 10^{-3} \text{ cm}^3/\text{mole}$  at  $0 \text{ K}$ .<sup>21</sup> If we assume that  $\mu_{\text{Mn}} = 0.6 \mu_B$  in  $\text{HoMn}_2$  (this is the average value from NMR

data and neutron diffraction studies and is in agreement with the results of magnetic measurements) we find that  $H_{\text{eff}}^{\text{Ho}} = 4.2 \times 10^6$  Oe. Using this value, we can estimate  $H_{\text{eff}}$  for the other  $\text{RMn}_2$  compounds from Eq. (3). It follows from our data (Fig. 8) that  $H_{\text{eff}}^{\text{Dy}} < H_{\text{cr}} < H_{\text{eff}}^{\text{Tb}}$ , whence  $5.25 \times 10^6 < H_{\text{cr}} < 6.3 \times 10^6$  Oe; thus,  $H_{\text{cr}}$  is considerably larger for the  $\text{RMn}_2$  compounds than for the  $\text{RCO}_2$  compounds where<sup>4</sup>  $H_{\text{cr}} = 1 \times 10^6$  Oe.

Thus, the model of the band metamagnetism of the manganese subsystem enables us to describe many features of the magnetic properties of various  $\text{RMn}_2$  compounds from a unified point of view and to compare them with the properties of other  $\text{RM}_2$  compounds. That is the principal advantage of this approach.

It should be noted, however, that this model is still hypothetical and, although there are many indirect indications of its validity, it has not been confirmed by direct experiments. In addition, there are data that cannot be fitted into such a simple model. These include the information in one of the earlier studies<sup>22</sup> on the noncolinear magnetic structure of  $\text{TbMn}_2$ , the problem of the nature of the recently discovered<sup>23</sup> low-temperature structure transformation in  $\text{YMn}_2$ , etc.

<sup>1</sup>We do not give the hysteresis loops of the investigated specimens here, but only note that they depend on the magnetic history of the specimen. This is specially pronounced in  $\text{TbMn}_2$ , as was noted earlier in Ref. 5. In Fig. 2 we give the magnetization curve of  $\text{TbMn}_2$  for the first application of the field.

<sup>2</sup>As our studies showed,  $T_C$  depends very strongly on the purity of the initial reagents in the case of  $\text{TbMn}_2$ . In the present paper we give the results for 99.93% pure grade Tb MD terbium and 99.85% pure electrolytic manganese.

- <sup>1</sup>K. H. Buschow, Rep. Prog. Phys. **40**, 1179 (1977).  
<sup>2</sup>H. R. Kirchmayr and C. A. Poldy, J. Mag. Mag. Mat. **8**, 1 (1978).  
<sup>3</sup>D. Gignoux, D. Givord, J. Laforest, R. Lemaire, and P. Molho, Proc. Conf. Phys. Mag. Mat. **1**, 96 (1980).  
<sup>4</sup>M. Cyrot and M. Lavagna, J. Phys. (Paris) **40**, 763 (1979).  
<sup>5</sup>E. A. Nesbitt, H. J. Williams, J. H. Wernick, and R. C. Sherwood, J. Appl. Phys. **34**, 1347 (1963).  
<sup>6</sup>A. Slebarski, J. Less-Common Met. **72**, 231 (1980).  
<sup>7</sup>S. K. Malik and W. E. Wallace, J. Mag. Mag. Mat. **24**, 23 (1981).  
<sup>8</sup>A. Tari, C. Larica, and J. Popplewell, J. Less-Common Met. **78**, P7 (1981).  
<sup>9</sup>A. S. Markosyan, Fiz. Tverd. Tela **23**, 1656 (1981) [Sov. Phys. Solid State **23**, 956 (1981)].  
<sup>10</sup>K. Shimizu, S. K. Dhar, R. Vijayaraghavan, and S. K. Malik, J. Phys. Soc. Japan **50**, 1200 (1981).  
<sup>11</sup>K. Hardman, J. J. Rhyne, S. Malik, and W. E. Wallace, J. Appl. Phys. **53**, 1944 (1982).  
<sup>12</sup>K. P. Belov, Magnitnye prevrashcheniya (Magnetic transitions), Fizmatgiz., Moscow, 1959 (Engl. Transl., Consultants Bureau, New York, 1961).  
<sup>13</sup>A. Slebarski and A. Chelkowski, J. Less-Common Met. **57**, 125 (1978).  
<sup>14</sup>D. Gignoux, F. Givord, R. Perrier de la Bathie, and F. Sayetat, J. Phys. (Paris) **F9**, 763 (1979).  
<sup>15</sup>B. Barbara, J. P. Giraud, J. Laforest, R. Lemaire, E. Sjaud, and J. Schweizer, Physics **86-88B**, 155 (1977).  
<sup>16</sup>A. S. Markosyan, Fiz. Tverd. Tela **23**, 1153 (1981) [Sov. Phys. Solid State **23**, 670 (1981)].  
<sup>17</sup>G. P. Felcher, L. M. Corliss, and J. M. Hastings, J. Appl. Phys. **36**, 1001 (1965).  
<sup>18</sup>D. Gignoux, D. Givord, F. Givord, and R. Lemaire, J. Mag. Mag. Mat. **10**, 288 (1979).  
<sup>19</sup>Françoise Givard and S. Shah Jayant, C. R. Acad. Sci. **274B**, 923 (1979).  
<sup>20</sup>B. Barbara, M. F. Rossignol, and M. Uehara, Physica **86-88B**, 183 (1977).  
<sup>21</sup>K. H. Buschow, Solid State Commun. **21**, 1031 (1977).  
<sup>22</sup>Lester M. Corliss and Julius M. Hastings, J. Appl. Phys. **35**, 1051 (1964).  
<sup>23</sup>I. Yu. Gaidukova and A. S. Markosyan, Fiz. Met. Metalloved. **54**, 184 (1982).

Translated by E. Brunner